Influence of the γ-Ray Dose on the Electrical Properties of Toluene Diisocyanate Mixed with Naturally Dehydrated Caster Oil Fatty Acids

F. A. Akraiam,[1] A. B. Elaydy,[2] A. A. Abed El-Latif[3]

[1]*Physics Department, Faculty of Science, Omar Al-Mukhtar University, El-Bieda, Libya*
[2]*Physics Department, Faculty of Science, Suez Canal University, Ismailia, Egypt*
[3]*Physics Department, Faculty of Education, Suez Canal University, Al-Arish, Egypt*

Received 17 April 2006; accepted 25 August 2006
DOI 10.1002/app.25952
Published online 20 July 2007 in Wiley InterScience (www.interscience.wiley.com).

ABSTRACT: Measurements of the alternating-current conductivity and direct-current conductivity before and after irradiation were studied for matrices composed of toluene diisocyanate mixed in four different ratios with dehydrated caster oil fatty acids. Different irradiation doses were investigated for all the samples. The alternating-current conductivity in the frequency range of 500–10000 Hz was found to obey the very well-known law $\sigma_{ac}(\omega,T) = A\omega^S$, where $\sigma_{ac}(\omega,T)$ is the alternating-current conductivity at angular frequency ω and temperature T and S is an exponent. The exponent decreased with increasing temperature for all compositions. A strong temperature dependence of the alternating-current conductivity and the exponent in the entire ranges of the temperatures and frequencies was reasonably interpreted with the correlated barrier-hopping model. © 2007 Wiley Periodicals, Inc. J Appl Polym Sci 106: 1847–1852, 2007

Key words: irradiation; matrix; polymerization; mixing; mechanical properties

INTRODUCTION

Thin and thick films of currently inorganic materials are growing in importance in many technical applications for insulation, isolation, and passivation in microelectronics.[1] We have made a matrix composed of toluene diisocyanate (TDI) as a base material mixed with dehydrated caster oil (DCO) fatty acids; this important plastic can be used to make various things such as color filters and insulation lacquers.[2,3] Moreover, it is a good insulating material, having a low dielectric loss and a good charge storage capacity. In recent years, considerable interest has been shown by different researchers in the effects of doping on the dielectric properties of various insulators.[4–6] No researchers until now have reported on these materials in the literature that we have used.

Parameters such as the dielectric constant, capacitance, and loss, as functions of the temperature and frequency, are considered the most convenient and sensitive tools for studying polymer structures. Also, γ radiation causes changes in the physical properties of materials. These changes are strongly dependent on the internal structure of absorbing substances. In this article, we report a matrix composed of TDI as a base material mixed with four different compositions, which has been studied for these purposes, and the results are discussed in detail.

Correspondence to: A. B. Elaydy (aelaydy@yahoo.com).

Journal of Applied Polymer Science, Vol. 106, 1847–1852 (2007)

EXPERIMENTAL

Sample preparation

A matrix composed of TDI was mixed with DCO fatty acids with different concentration ratios, as mentioned previously, on a roll mill under typical industrial mixing conditions (Table I).[7] The investigated samples were shaped into soft disks during a heat treatment under atmospheric pressure at 85°C for 60 min. All the products of this mixture were very stable, greenish, odorless, and not transparent. Only samples of very high quality from this matrix were selected and used for the electrical conductivity and other measurements. All samples were thermally aged at 60°C for 20 days before irradiation to ensure their structural stability. A ^{60}Co γ source (model GB150 type B), manufactured by the Atomic Energy Agency of Canada and located at the National Center for Radiation Research and Technology (Cairo, Egypt), was used as an irradiation source for all samples. The measured thickness of the produced films was around 0.21 mm. The selected films were divided into four groups labeled TD1, TD2, TD3, and TD4, which correspond to ratios of TDI to DCO fatty acids of 1/1, 1/1.5, 1/2, and 1/2.5, respectively, as shown in Table I.

TABLE I
Experimental Values for the Matrix of TDI with Different Amounts of DCO

Material	Sample	Ratio (wt %)
TDI/DCO	TD1	1/1.0
TDI/DCO	TD2	1/1.5
TDI/DCO	TD3	1/2.0
TDI/DCO	TD4	1/2.5

Electrical measurements

The samples composed of TDI and DCO fatty acids were cut from the original bulk materials into disks 1 cm in diameter. These disks were coated very well on both sides with silver paint to ensure good electrical contact between the two electrodes of the sample holder in the cell. The cell used for the electrical measurements consisted of four stainless steel rods 10 cm long, the top and bottom bases of which were disks, and there were also many small ceramic parts for insulation. The samples within the cell were put inside an electrical furnace with a digital thermometer just in contact with the samples to measure just the sample temperature without any temperature gradient. The accuracy of the temperature measurement for all the samples was better than 0.2 K. The temperatures varied over the range of 293–500 K with a temperature control of ±0.5 K. Very fine copper wires were cemented onto both surfaces of the holder with paint, and then the samples were mounted on a sample holder.

Measurements of the direct-current conductivity were carried out with a Keithley 616 digital electrometer at room temperature from current–voltage relationships (Table II). The direct-current electric conductivity values increased with an increasing ratio of DCO fatty acids in all the samples. Although the measurements of the alternating-current conductivity at angular frequency ω and temperature T [$\sigma_{ac}(\omega,T)$] were made with a HiTester type 3531 Z RLC bridge, the effective dielectric constant of all these samples was evaluated from the experimental values of both the capacitance and loss factor. The temperature could be varied over the range of 293–500 K with a temperature control of ±0.5 K, and the temperature was increased continuously with an electric variance apparatus unit. The measurements for all frequencies were performed with the same RLC bridge in a frequency range of 0.5–10 kHz.

Such behavior is inconsistent with the quantum mechanical tunneling model,[10(b),13] which predicts either a temperature-independent exponent (S) or an exponent that is an increasing function of temperature.[8] The only model that appears to be consistent with these data is the correlated barrier hopping model.[9] In the correlated barrier hopping model, the temperature dependence of S is predicted to be approximately

$$S = 1 - 6kT/W_M \quad (1)$$

where W_M is the maximum barrier height and k is the effective dielectric constant.

Equation (1) shows that exponent S increases with decreasing temperature T, as observed for these data. However, the results are in qualitative agreement only. This correlated barrier hopping model assumes that carrier motion occurs by means of hopping over the potential barrier separating two defect centers. The real part of $\sigma_{ac}(\omega,T)$ derived for this model with a random distribution of centers[10] is given by the following equation:

$$\sigma(\omega, T) = n\pi^2 N N_c k\omega R_\omega{}^6/24 \quad (2)$$

where $\sigma(\omega,T)$ is the conductivity at angular frequency ω and temperature T, n is the carrier density, N is the total density of participating levels, N_c is the number of carriers, and R_ω is the resistance at angular frequency ω.

Elliot[8(a)] suggested that the energy required to remove two electrons simultaneously from the D^- state was given by Davis and Mott,[11] who stated that

$$W_m = E_g - W_1 + W_2 \quad (3)$$

where W_m is the maximum energy required to remove two electrons from a D^0 centre, E_g is the band gap and W_1 and W_2 are approximately the distortion energies associated with the neutral D^0 and D^- states, respectively. Because the electron does not bond with the lone orbiting pair, the small acceptor energy is also negligible.[8(a)] Therefore, W_1 and W_2 have roughly the same magnitudes.

RESULTS AND DISCUSSION

Effects of DCO on the conductivity matrix

Measurements of the direct-current conductivity were carried out with a Keithley 616 digital electrometer at room temperature, as shown in Table II.

TABLE II
Direct-Current Conductivity Values for TDI/DCO Samples Before Irradiation at Room Temperature

Sample	t/A (m^{-1})[a]	R (Ω)[b]	σ [(Ω m)$^{-1}$][c]	σ_0 [(Ω m)$^{-1}$][d]
TD1	35.377	3.660×10^{11}	9.666×10^{-11}	2.056×10^{-6}
TD2	33.805	2.564×10^{11}	1.319×10^{-10}	7.378×10^{-6}
TD3	73.506	2.570×10^{10}	2.860×10^{-11}	0.129×10^{-6}
TD4	9.906	1.990×10^{9}	4.978×10^{-9}	5.604×10^{-6}

[a] Thickness/area ratio.
[b] Resistance.
[c] Conductivity [$\sigma = 1/R \times (t/A)$].
[d] Pre-exponential factor.

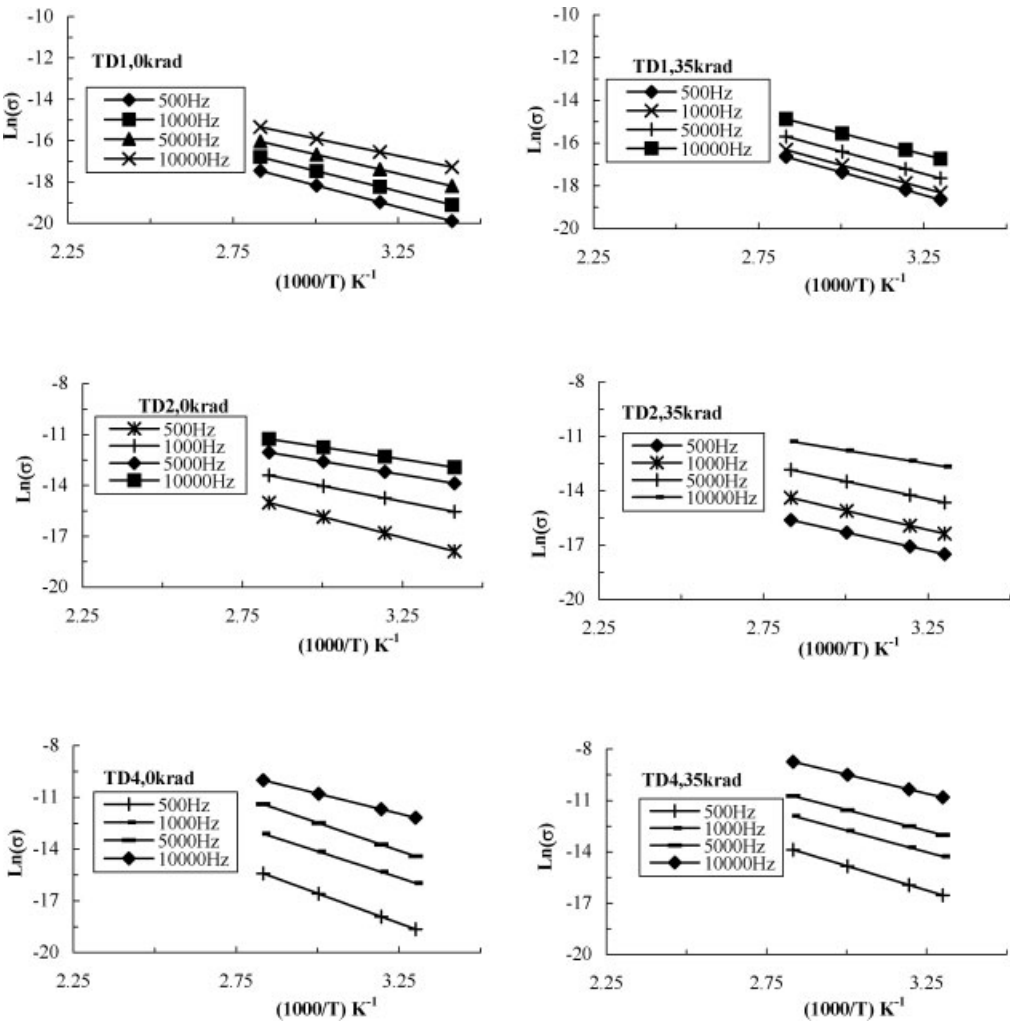

Figure 1 Temperature dependence of the alternating-current conductivity (σ) for irradiated and unirradiated TDI/DCO composites at different frequencies.

We deduced from the values of the current–voltage relationship curves the nonohmic coefficients for all the samples. We also noticed from this table that the direct-current electrical conductivity increased from 9.666×10^{-11} to 4.978×10^{-9} $(\Omega\ m)^{-1}$ with increasing ratios of DCO fatty acids to TDI in all the samples. Although this a relative increase, the materials are still insulators.[12]

Activation energy characteristics at different γ-ray doses

The values of the activation energies were derived from the slopes of the plots of Figure 1, which relates the alternating-current electrical conductivity to the absolute temperature and follows the very well-known Arrhenius law:

$$\sigma(\mathrm{S/m}) = \sigma_0 \exp\{-[E_a/(k_B T)\} \quad (4)$$

where σ is the conductivity, σ_0 is a pre-exponential factor depending on the material, E_a is the activation energy for the conduction mechanism, T is the absolute temperature used for the samples, and k_B is Boltzmann's constant. The activation energies of all samples were estimated with the slopes of the aforementioned plots ($E_a = -\text{Slope} \times k_B$). The calculated data for the activation energies are summarized in Table III. The activation energies for all the samples versus the DCO fatty acid contents are shown in Figure 2. Table III shows that the activation energy

TABLE III
Activation Energies for Samples of TDI/DCO Fatty Acid Mixtures

Sample	TDI/DCO ratio (wt %)	Activation energy (eV) 0 krad	20 krad	25 krad	30 krad	35 krad
TD1	1/1.0	0.019	0.025	0.036	0.081	0.163
TD2	1/1.5	0.167	0.148	0.209	0.229	0.290
TD3	1/2.0	0.171	0.298	0.339	0.402	0.438
TD4	1/2.5	0.173	0.386	0.440	0.507	0.553

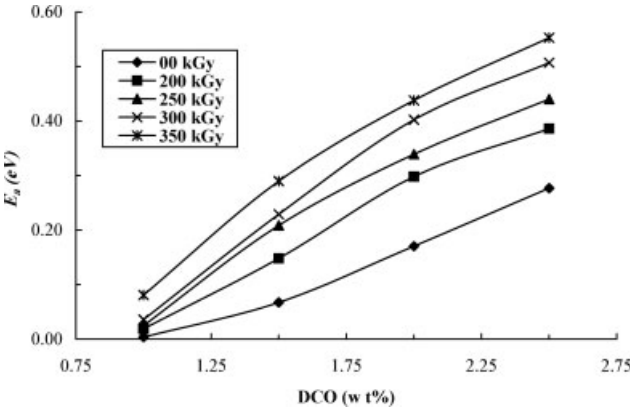

Figure 2 Relationship between DCO and its activation energy (E_a).

increases with an increasing amount of DCO fatty acids and a decreasing dose. The steady-state values for these samples become more meaningful if they are presented as Arrhenius plots according to the aforementioned law, from which the activation energy was obtained. The absolute values of the activation energy varied from one sample to another, depending on the DCO ratio in all the samples.

Temperature dependence of the alternating-current conductivity (σ_{ac}) at different γ-ray doses

The temperature dependence of $\sigma_{ac}(\omega,T)$ for the matrix composed of TDI as a base material mixed with DCO fatty acids versus $1000/T$ is shown in Figure 1. In the high-temperature region (271 K), the samples exhibited activated conduction with activation energies varying from 0.123 to 0.579 eV for all doses. The increase in the activation energies with increasing concentrations could be due to an increasing band gap. The band gap increased with an increasing amount of DCO fatty acids.[13]

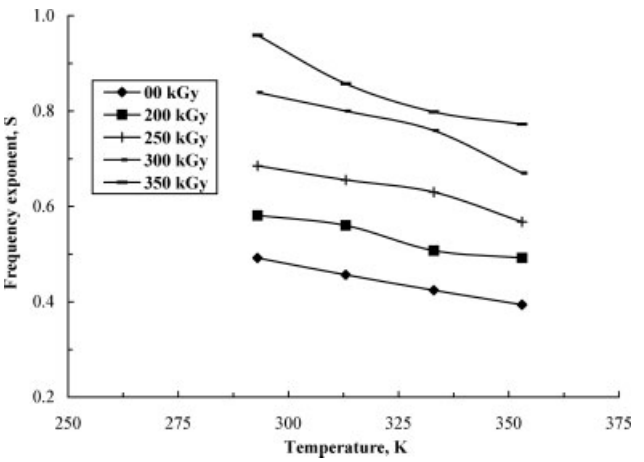

Figure 3 Relationship between the frequency exponent and temperature for TD1 specimens.

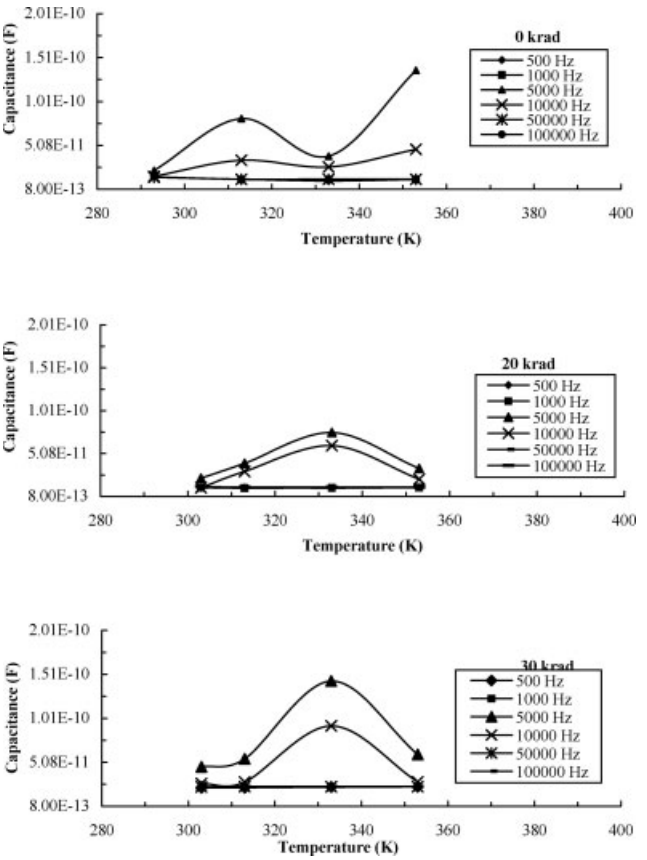

Figure 4 Temperature dependence of the capacitance of TD1 composites before and after irradiation at different frequencies.

The σ_{ac} values for the different samples showed a strong frequency dispersion in accordance with the well-known relation $\sigma_{ac}(\omega,T) = A\omega^S$. The conductivity dependence of exponent S, obtained for these data for sample TD1, is shown in Figure 3. S increased slightly with increasing σ_{ac}.

Variation of the sample capacitance with the temperature at different γ-ray doses

The variation in the capacitance of the samples with the temperature at various frequencies for unirradiated and irradiated states was studied systematically. Figures 4 and 5 depict the change in the capacitance for samples TD1 and TD3, respectively. The irradiated samples showed a slight increase in the capacitance at 310 K, which then decreased rapidly up to 335 K and then increased again to reach a maximum. Thereafter, a sharp increase in the capacitance was observed for all frequencies.

Figure 5 shows that for specimens irradiated with 25 and 35 krad, unlike the unirradiated specimens, an

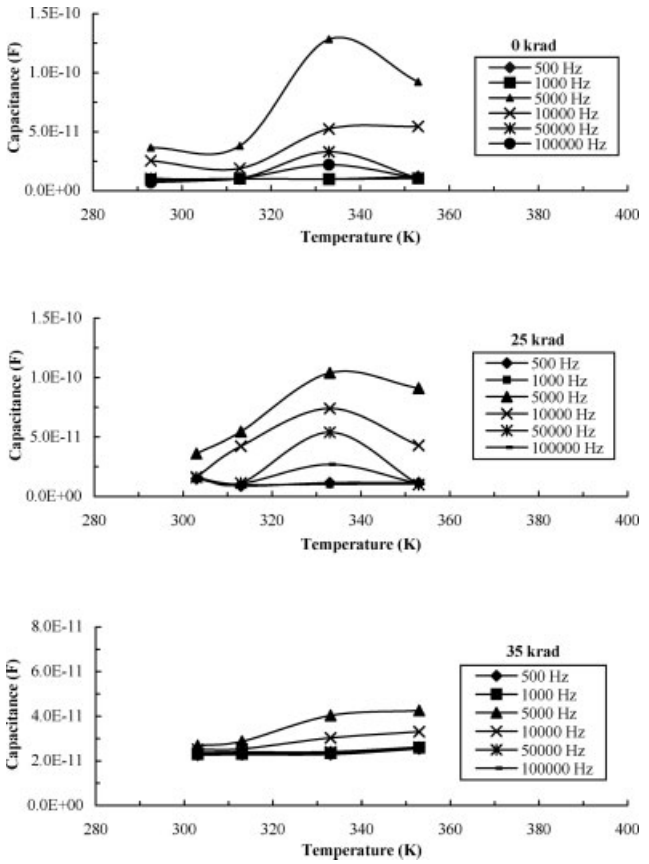

Figure 5 Temperature dependence of the capacitance of TD3 composites before and after irradiation at different frequencies.

increase in the capacitance occurred even from room temperature. This value reached, without a shift, a maximum at 355 K for all frequencies. In both the unirradiated and irradiated cases, the capacitance decreased with an increase in the frequency.

σ_{ac} as a function of frequency at different γ-ray doses

Figures 6 and 7 illustrate the experimental results for $\sigma_{ac}(\omega,T)$ for the unirradiated and irradiated samples (TD1 and TD3) studied at different temperatures and different frequencies. The plots in both figures were determined with the least-square fitting method. The alternating-current conductivity at angular frequency ω [$\sigma_{ac}(\omega)$] slowly increased with the frequency increasing in the range of 500–10,000 Hz. This linear relation indicated that the alternating-current component of the conductivity had a frequency dependence:

$$\sigma_{ac} = \text{Constant} \times \omega^{S} \quad (5)$$

The universal character of frequency-dependent conductivity is preserved in a wide range of materials, including insulating materials. However, the slowly

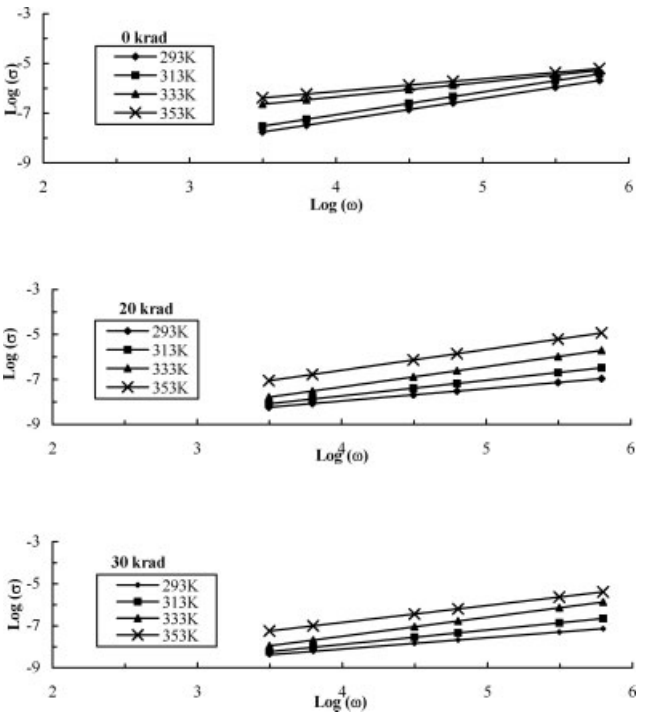

Figure 6 Variation of the logarithm of the conductivity (log σ) with the logarithm of the angular frequency (log ω) for TD1 samples before and after irradiation at different temperatures.

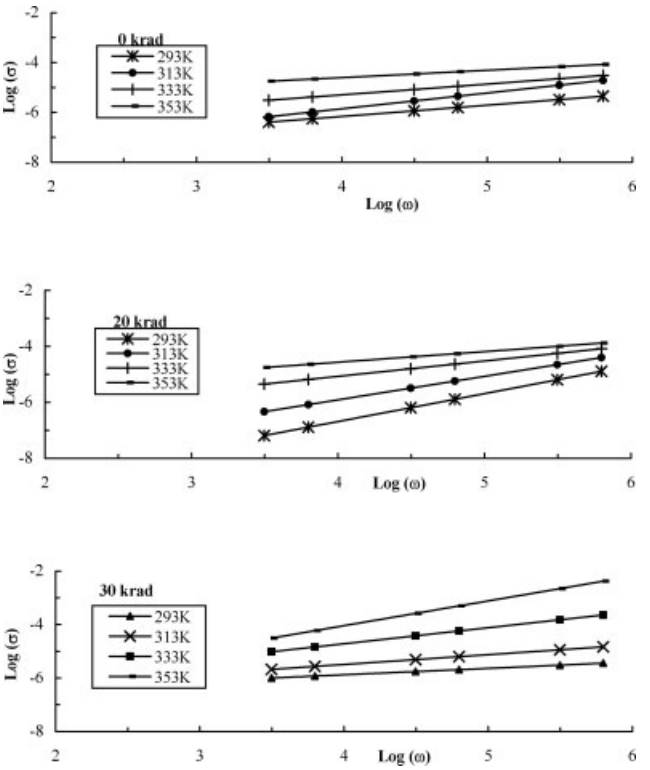

Figure 7 Variation of the logarithm of the conductivity (log σ) with the logarithm of the angular frequency (log ω) for TD3 samples before and after irradiation at different temperatures.

variable conductivity at low frequencies can be attributed to a strong dispersion of both the real and imaginary components of the dielectric permittivity.[14] There is not a big overall change in $\sigma_{ac}(\omega)$ with increasing DCO fatty acids in the samples.

CONCLUSIONS

The effects of γ irradiation on a matrix composed of TDI mixed in different ratios with DCO fatty acids were very well studied. Thick films of the matrix were fabricated with a roll-mill technique. The samples were exposed to a γ-radiation source for doses of 20, 25, 30, and 35 krad. The characteristic data were recorded after a fixed exposure time. The electrical properties of these samples were somewhat affected by exposure to γ radiation. For example, the σ_{ac} values increased as the radiation dose was increased. Also, these experimental results indicated that some of the examined samples could withstand severe radiation effects and could be used as electrical insulators. Also, an increase in the capacitance of the samples with increasing temperature may have been due to the alignment/rotation of the dipole temperature.

References

1. Macon, W. H. In Plastic Insulation; Bruins, P., Ed.; Wiley-Interscience: New York, 1968; p 141.
2. Gowarikar, V. R.; Viswanathan, N. V.; Sreedhar, J. Polymer Science; Wiley-Eastern: New Delhi, India, 1988.
3. Moore, W. R. An Introduction to Polymer Chemistry; University of London Press: London, 1967.
4. Abd-Lefdil, M.; Laplaze, D.; Cadene, M. Solid State Commun 1990, 73, 81.
5. Turucu, R. Phys Status Solidi A 1990, 119, K121.
6. Pillai, P. K. C.; Gupta, A. K. J Mater Sci Lett 1983, 2, 397.
7. Gwaily, S. E.; Nasr, G. M.; Badawy, M. M. M. M. Egypt J Sol 2001, 24.
8. (a) Elliot, S. R. Philos Mag 1977, 36, 1291; (b) Elliot, S R. Philos Mag B 1978, 37, 135; (c) Elliot, S R. Philos Mag B 1978, 37, 553; (d) Elliot, S R. Philos Mag B 1978, 38, 325; (e) Elliot, S R. Philos Mag B 1979, 40, 507; (f) Elliot, S R. J Noncryst Solids 1980, 35, 855.
9. Lakatos, A. I.; Abkowitz, M. Phys Rev B 1971, 3, 1791.
10. (a) Pollak, M. Phys Rev A 1964, 133, 564; (b) Pollak, M Philos Mag 1971, 23, 519; (c) Pollak, M J Noncryst Solids 1972, 11, 1; (d) Pollak, M. Garmisch, Germany, 1974; p 127; (e) Pollak, M. Leningrad, Russia, 1976; p 79; (f) Pollak, M Philos Mag 1977, 36, 1157.
11. Davis, E. A.; Mott, N. F. Philos Mag 1970, 22, 903.
12. Kamel, R. Atomic Theory of the Solid State; 1984; p 127.
13. Austin, I. G.; Mott, N. F. Adv Phys 1969, 18, 41.
14. Jonscher, A. K. Nature 1977, 267, 673.